Model-Free Multi-Camera Calibration By Graph Pyramid Using 360° Pattern

Majid Banaeyan[1]
Pattern Recognition and Image Processing Group 193/03, TUWien, Vienna, Austria

Abstract
Camera calibration should be easy to perform on the one hand and provide robust results on the other hand. These requirements motivate the proposed, "unusual" approach for multi-camera calibration. For camera calibration, common methods assume a geometrical model to correct distortion. Here, however, the proposed method introduses an approach that does not make any assumptions about the projection model of the lens and its parameters and thus allows nearly arbitrary distortions. This calibration procedure employs a special 360º pattern including different markers and fractal shapes in different resolutions which applicable in particular to multi-camera setups. For such multi-camera setups, not only a calibration is needed for each camera, but the individual images have to be aligned to fit together in a final image mosaic. Image alignment is usually considered a separate problem from distortion correction and thus handled separately. The proposed approach, however, combines distortion correction and image alignment in a single procedure. This new approach employs graph pyramids to perform this registration problem and entails several advantages. First, it does in one procedure both distortion correction and image alignment using a specific 360º pattern. Second, it includes highly parallelized processes meants that individual images are prepared by the cameras themselves and the computational cost at a central processor is reduced. Finally, there is no need to detect key points and solve the correspondence problem in order to do image stitching.

Keywords: Multi-Camera Calibration, Model-free, Graph Pyramid, 360º Pattern, Image Processing.

1- Majid Banaeyan is supported by Pattern Recognition and Image Processing (PRIP) group via PRIP-Club.

1. Introduction

Camera calibration establishes a mapping between 3D real-world coordinates of an observed scene and the corresponding 2D coordinates in the acquired image. This mapping may be de_ned by parameters of a projection model. Generally, we distinguish extrinsic parameters (defining the pose of camera) and intrinsic parameters (depending on the internal nature of the lens and the sensor) [1].

1.1. Camera Models

The pinhole camera model is the most basic camera model. It is used as an approximation within various computer vision applications [2]. In order to improve the calibration accuracy, the pinhole model is combined with lens distortion models [3, 4]. However, for lenses that produce a high visual distortion, e.g. wide-angle lenses with a field of view (FOV) larger than 180º, the pinhole model is not suitable. For instance, cameras equipped with fish-eye lenses with extremely short focal length provide hemispherical images. Their geometry cannot be described based on central perspective projection [5]. Straight lines in the scene appear as curves in images captured using such lenses [3] and require non-linear transformations in addition to the projective geometry [6]. Therefore, alternative projection models such as equidistant, equisolid-angle, orthographic and stereographic projection geometries have been used to compensate this deficiency [7, 4]. The main idea here is to first find an ideal mapping using a sylindrical projection and then apply a subsequent correction. In [8] a similar model based on the spherical projection is created to develop the epipolar geometry for fish-eye lenses and to solve the triangulation problem using the least-square method. In [9] the mapping between pixel coordinates and 3D rays in camera coordinates is considered a linear combination of non-linear functions of the image coordinates. The calibration procedures presented in [10] and [11] assume a radially symmetric distortion to calibrate fish-eye lenses, whereas the procedures presented in [12] and [13] use the knowledge about straight lines in the scene and force them to be straight in the image as well. Further techniques are based on Hough transform [14] and circle fitting [4] or use first order Taylor expansion to derive an inverse function for radial distortion [15]. All parametric methods depend on the accuracy of the chosen projection model and the degree to which this model approximates the actual projection of the lens. For non-standard lenses, deviations from the ideal projection can be large and often lead to unstable approximations [16].

Contrary to the calibration procedures with parametric models, non-parametric calibration methods aim at providing procedures independent of the type of camera or lens. While parametric camera models are state-of-the-art for many applications, non-parametric camera models have been much less discussed in literature. The main idea of these approaches is to assign a line of sight in 3D to every camera pixel [17, 18]. In [18] a set of virtual sensing elements called raxels is used to perform mapping from incoming scene rays to photosensitive elements of the image detector. In [17] a general concept for this type of calibration is described. However, the method does not yield satisfying results for non-central catadioptric cameras and the general algorithm also does not work for perspective cameras. Some authors call it 'generic' calibration [17].

1.2. Multi-Camera Setups

Multi-camera calibration denotes the process of determining the relative poses of all cameras in the setup in a global coordinate system. There are different multi-camera setups which vary in configuration. Generally, there are three categories: inward-looking cameras, outward-looking cameras and camera networks: Inward-looking cameras share a common FOV, for outward-looking cameras the FOVs of the individual cameras do not overlap and in camera networks, some cameras share a FOV, but not all FOVs overlap [19]. Camera pose determination can be performed employing a family of linear methods [20]. Moreover, object silhouettes (Shape-from-Silhouette) may be used to estimate the epipolar geometry of the cameras [21].
For the calibration of a network of cameras, objects are used to first determine the relative transformation between cameras with shared FOV. By utilizing bundle adjustment [22], the globally consistent localization is obtained. For this purpose, many methods are based on the "wand dance procedure" [23, 24] which uses a wand with one, two [25] or more [26] LEDs as a calibration object. Usually, the wand is moved to obtain more point correspondences [25]. For accurate results, the cameras must be precisely synchronized to capture images at the same time [27, 25]. In [27] a laser pointer was used to perform the self-calibration. Direct Linear Transformation (DLT) methods [28] can be used to estimate initial parameters for the first step of calibration [24]. Distributed camera networks may also be calibrated by defining the vision graph and using an algorithm based on belief propagation [29].
Outward-looking cameras do not have a common FOV [30, 31, 32]. However, for cameras with wide angle lenses, an overlap in the FOV may appear, which is the case for the setup is proposed in this paper. In case parts of the FOV overlap, the pose between cameras can be estimated using the rigidity constraint of the rig [30] or the rotation averaging approach [33] which uses bundle adjustment to improve accuracy [22, 31]. Furthermore, a planar mirror may be used to describe the camera pose [32]. Because of these variations in configurations of multi-camera setups, different calibration methods are commonly used for these categories and suitable applications may vary. Inward-looking setups are useful in 3D reconstruction, whereas outward-looking configurations are suitable for image stitching [34, 35] and thus the creation of panoramic images [36].

1.3. Stereo Cameras

Stereo cameras are considered inward-looking setups as well. In stereo vision, the aim is to determine depth information from at least two images with overlapping FOV. For this purpose, corresponding points are determined and a disparity map is computed. Image rectification reduces the correspondence problem from a search in 2D space to a search in 1D along epipolar lines. Rectification needs re-sampling and consequently comes with a loss in resolution. Stereo disparities can be determined based on either local or global constraints [37, 38]. Approaches such as block matching [39], gradient-based optimization [40] and feature matching [41] are considered local methods whereas dynamic programming [11],intrinsic curves [43], and graph cuts [44] represent global methods. Moreover, window-based approaches [38] may use fixed [45] or adaptive [46] search windows.
Contrary to the calibration methods for multi-camera setups described above, the paper here proposes a camera network calibration approach for which correspondence problems are not needed to be solved. Instead, it establishes a mapping to a global target coordinate system using image segmentation. final panorama image is handled by extrapolating a weighted warp from overlap regions of the image to non-overlap regions and by applying a constrained relaxation step of the full panorama frame to a reference projection.

2. Model-free Single Camera Calibration

In our proposed calibration method, the target coordinate system is defined by the calibration pattern used. This method therefore allows for many different target coordinate systems including non-standard ones, since their patches may be arranged in an arbitrary order as long as a certain coordinate may still be associated with every region (patch) of the calibration pattern. At the current stage a rectilinear coordinate system configured cylindrically around a multicamera setup is considered, but a spherical configuration may as well be an option.
The calibration procedure in the paper is a mapping between the coordinate system of the input image and the target coordinate system of an undistorted (calibrated) image. The idea is to employ image segmentation to obtain this mapping: In a graph pyramid [47], each pixel in the base level is represented by a vertex and the vertices of neighboring pixels are connected by an edge. By consecutive contraction of edges pixels with similar values are merged into regions which are represented by vertices on a higher level - each level of such a pyramid is represented by a region adjacency graph (RAG) of decreasing detail (see Figure 1).

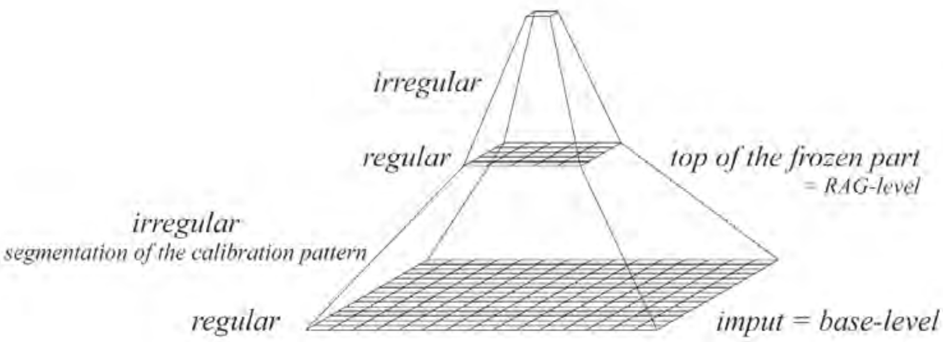

Fig1. Construction of an image pyramid

For our purpose, the aim is to segment the image of the calibration pattern (e.g. a checkerboard pattern) using a graph-pyramid based approach until reaches the level where for each patch of the pattern, its pixels are merged into a single region represented by a vertex: this level is called the "RAG level". The identification of corresponding regions in the input and the target pattern is straightforward since the number of patches is the same and can thus be measured by counting in order to define the mapping at the respective level of the graph pyramid. To obtain a transformation on pixel-level, the high-level information is propagated down to the base level of the pyramid using the segmentation history that is stored in the canonical pyramid representation [22]. The rest of the steps is explained in the next section.

3. Model-free multi-camera calibration

The proposed calibration algorithm works for arbitrary arrangement of the cameras which the union of their field of views (FOVs) covers the 360º space around them. For the sake of simplicity and better explaining the proposed method, a specific arrangement of six cameras locating around a circle with equal angular distance between each one (60º) is considered. The Fig.2 shows such multi-camera system. In such an arrangement, the FOV for each camera is 180º and each part of the pattern can be seen by at least two adjacent cameras. However, there are some parts of the pattern which are seen by three cameras. These overlapping areas are illustrated in Fig.2.

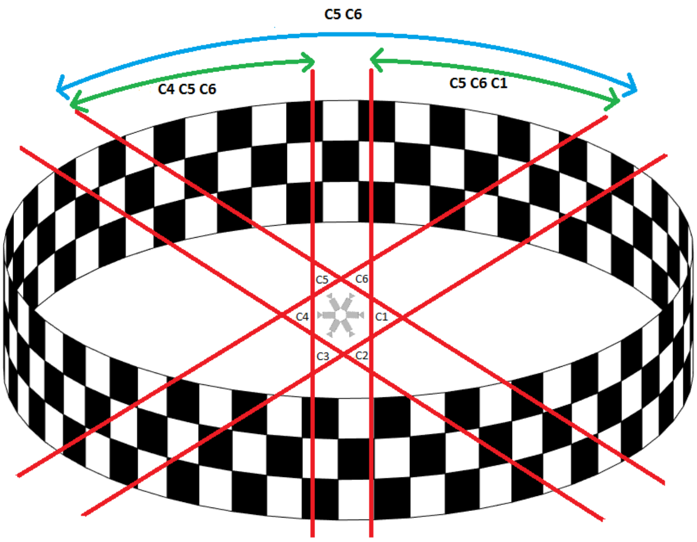

Fig2. A multi-camera system with 6 cameras (C_i ,i=1,2,..,6). The Blue FOV shows the overlapping between two cameras and the Green FOV between three ones.

3.1. Correspond the image to the real world

In contrast to the common methods for calibrating a camera, here no specific model for the lens of the camera is assumed. Indeed, the distortion of the lens is assumed to be an unknown non-linear function. At this point, the task of calibration is to correspond every individual pixel of the 2D image to its correspondence in the 3D read world. Usually very wide FOV lenses result in a high distortion on the side of the image and less in the center. As a result, the objects aligned in the side of the camera become smaller and highly deformed and those objects around the center are highly magnified. Fig.3 shows such distortion in a fish eye lens.

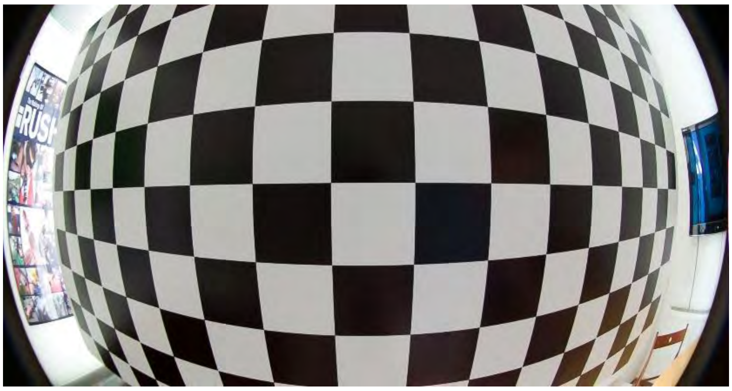

Fig3. An example of a checkerboard image taken by the very wide fish-eye lens. The patches are located on the sides become smaller and more distorted and those in center magnified.

Having said that, no matter what is the distortion of the lens, the light beams traverse a unique line from the outer lens into the 3D world. In other words, there is a unique point for each pixel of the image plane projected to the corresponding point in space (see Fig4.). Therefore, the task of calibration is to define such correspondence matching.

Generally, in camera calibration systems a known pattern, e.g. a black and white checkerboard, is shown to the camera and then the camera identifies the matching of some robust features (usually corners) for each corresponding feature. Now, having multiple correspondences between two set of virtual and real points, by assuming a predefined mode for the lens, the calibration is performed.

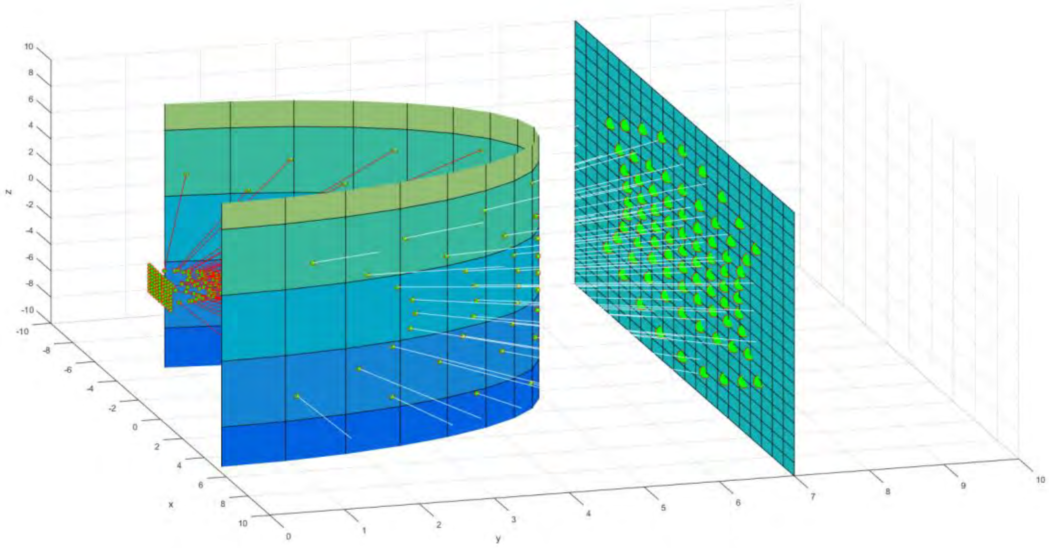

Fig4. The light beams traversing straight lines from the outer lens into the 3D space

Generally, there are two types of camera models for the lenses. The standard models which assume pinhole projection and the non-standard ones that consider the radial distortion. Normal cameras belong to former and the fish-eye ones - to latter. Now, consider, for example, the fish-eye cameras. By assuming the predefined radial distortion model, after matching the corresponding points, all the rest points employ the same formula to be projected. Therefore, in the cases that there are non-symmetrical distortions, like unwanted movement of lenses, or having non-symmetrical distortions, the non-corresponding points cannot correctly be matched and the calibration fails.

In proposed calibration algorithm, we do not assume any predefined model and instead the correspondence matching task is performed by using the specific 360º calibration pattern. Fig.5 shows the 360º black and white pattern. The proposed pattern encodes uniquely the 3D space around the set of the cameras. It includes specific markers which not only define the origin of the pattern, but also assign the relative coordinate into each individual patch of the checkerboard. In fact, each camera when sees a part of the pattern in its FOV, can immediately define where its location in relative to all other patches is.

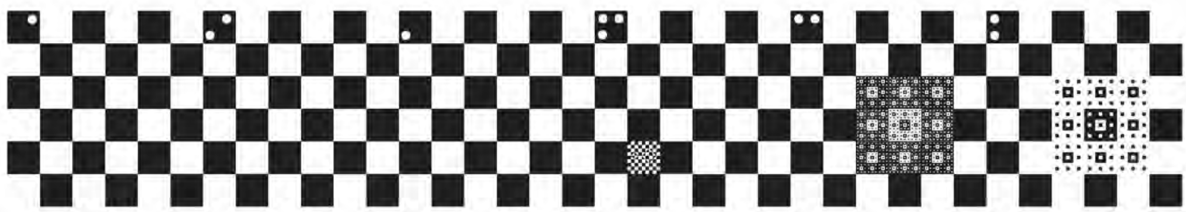

Fig5. The specific 360º blach and white pattern

Beside the markers, there are some patches which have special fractal pattern in their inside. These patches paly the refinement procedure of calibration as are explained later.

3.2. Identifying the corresponding part of the pattern in each individual camera

Based on the arrangement of the cameras in a multi-camera system, the overlapping areas is defined. Here, since the cameras are located in a symmetrical constellation and since they have the same resolution, they divide the image plane into 6 rectangles which all together create the 360º image. By using the 360º pattern, the corresponding matching problem between the two adjacent cameras changes into the easily just counting the patches.

3.3. Graph pyramid segmentation algorithm

To detect the correspondence points of each individual camera and the 3D space, the graph segmentation algorithm for the binary pattern is employed. In such segmentation, first the primal graph of the image is created at the first level of the irregular pyramid. Second, by consecutively contracting the contraction kernels step by step the next levels are built. Finally, the region adjacency graph (RAG) at the top of the pyramid is represented. Such a RAG has the property that each of its node is consider as one patch of the checker board [48].

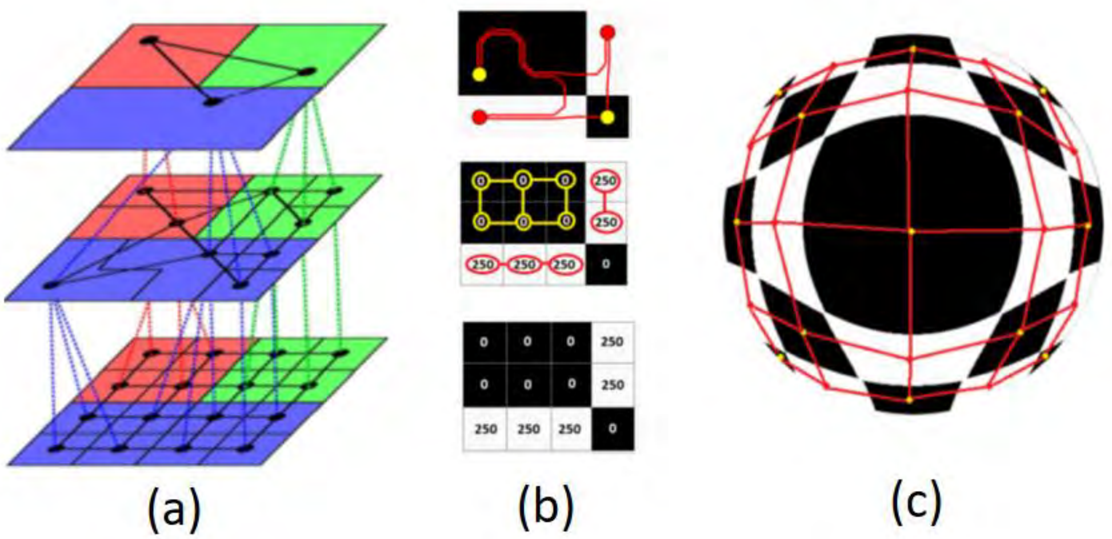

Fig6. (a) an irregular graph pyramid. (b) Image segmentation in a three levels pyramid. (4) a region adjacency graph (RAG) at top of the pyramid. Each node of the graph represent a distorted patch of the checker board.

3.4. Finding the correspondences

After segmenting the image each node of the resulted graph on top of the pyramid represents a unique patch of the checker board. Now, since there are special markers in the 360º pattern, one can simply find outs the coordinate of each patch by just counting patches in between till reaches to the pre-defined origin. The markers and the fractal shapes are illustrated in magnifid size in Fig.7.

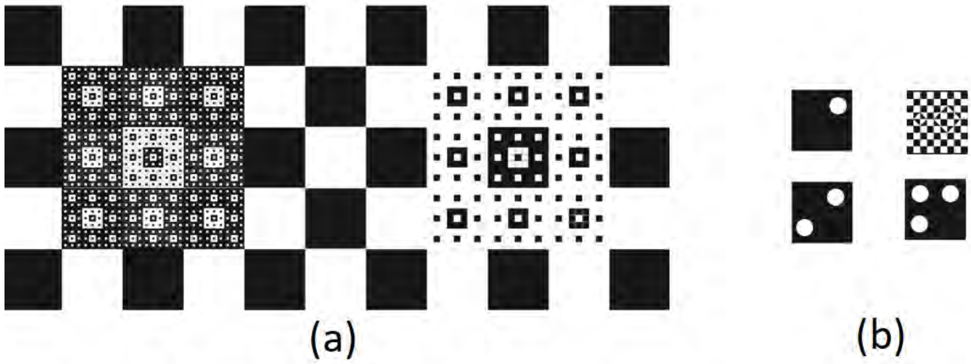

Fig7. (a) the fractal shapes in different resolutions. (b) the markers inside the 360º pattern

3.5. Refining the calibration

The 360º pattern has special fractal shape patches. The main property of the fractals is that they generate the same shape in different scales or different positions. Therefore, in the pattern as it sees in Fig. two fractals in two different scales are designed. Every normal patch in such pattern has uniform region inside its patch. This means that the corresponding points of the resulted graph for each normal patch has 4 points from the world. Hence, the points between the corners have not any correspondence. Now, at this point, by rotating the pattern around the multi-camera system each time there is a new pattern in the FOV of the cameras. This means that whenever the position of the high resolution (fractal) patches are changed, a new part of the space get a high number of corresponding points. Therefore, after rotating the pattern in a few times, the space receives the corresponding matching points as the high resolution in the fractal patch. Note that, if the pattern is fixed one can use the 360º turn-table to put the camera in center and rotate the multi-camera system instead of the pattern.

4. Discussion and implementation.

Following an important problem exists in cameral calibration explaines and the solution is discussed. Then the next part the results are summerised.

4.1. Solving the problem of corresponding by using DT

One of the common problem of the camera calibration is to define exactly where the location of a corner is. As it mentioned before, in a very wide FOV, the patches that are located in the side of the image receive much more distortion (see Fig.8). As the result, a single corner which is between two diagonal patches becomes two distinguish points. Therefore, the calibration may fail or becomes less accurate. In the proposed algorithm this multi-corners cause that the two adjacent one-color patches connected to each other and hence are considered as a one patch. Therefore, to avoid such situation, the algorithm computes the distance transform (DT) inside each individual patch of the pattern. This results in detecting the center of the patches instead of the corners. By using DT every patch has its local extremum which is uniquely identified its patch (Fig.9).

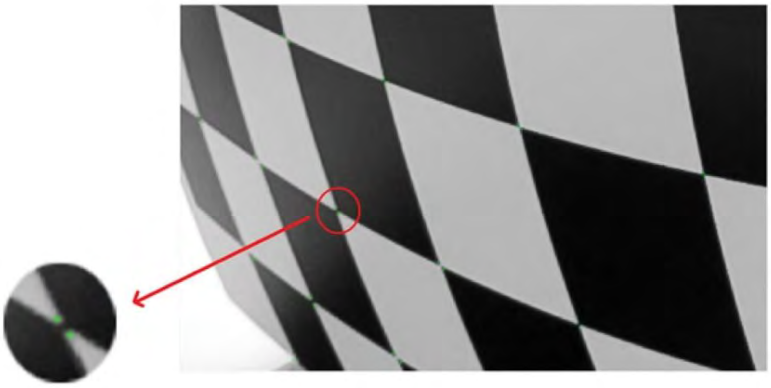

Fig8. The multi-corner detection problem in side of the high distorted image

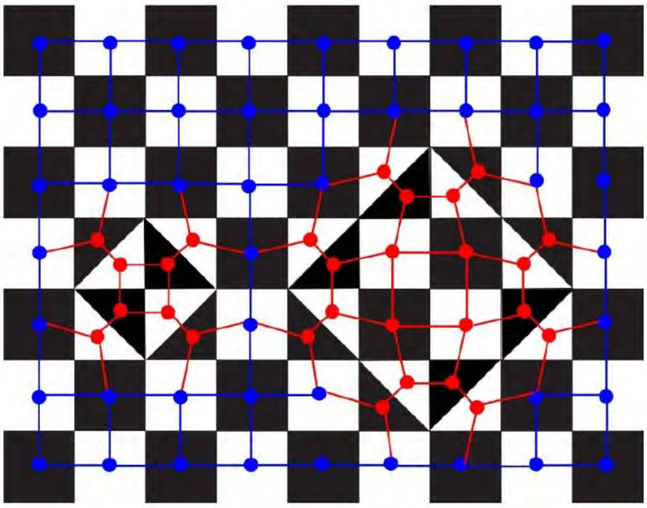

Fig9. Using distance transform (DT) to shift the corners to the center of the patches

4.2. Implementation

The 360º cylindrical pattern is shown in Fig.10. It covers the area around the camiera rig and there are 6 cameras in the arrangement. The diameter of the pattern in cylindrical situation is 100 cm. Each fish-eye lens has 200º FOVand the resultion of each camera is 7800 by 3600 pixel. Size of the square patch in the pattern (read 3D world) is equal to 9 cm. The standart and little-planet view of the resulted stitched 360º image sre shown in Fig.11 and Fig.12, respectively.

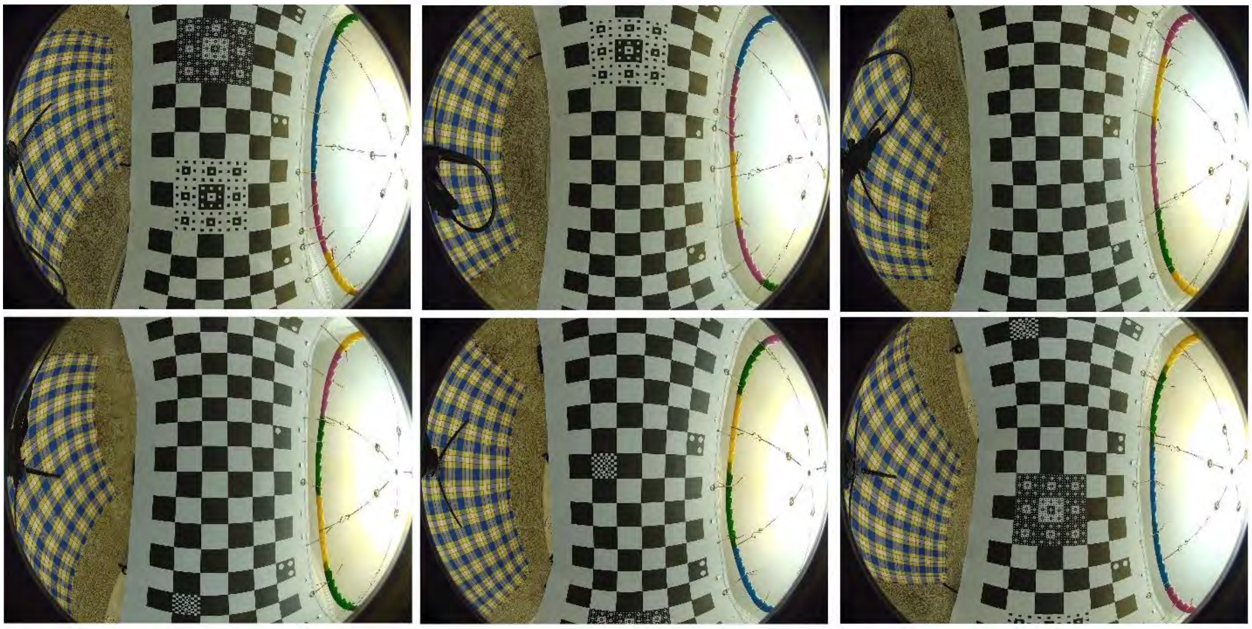

Fig10. The 6 fish-eye frames corresponding to 6 cameras in the multi-camera system.

Fig11. The stitched 360° image in standard view

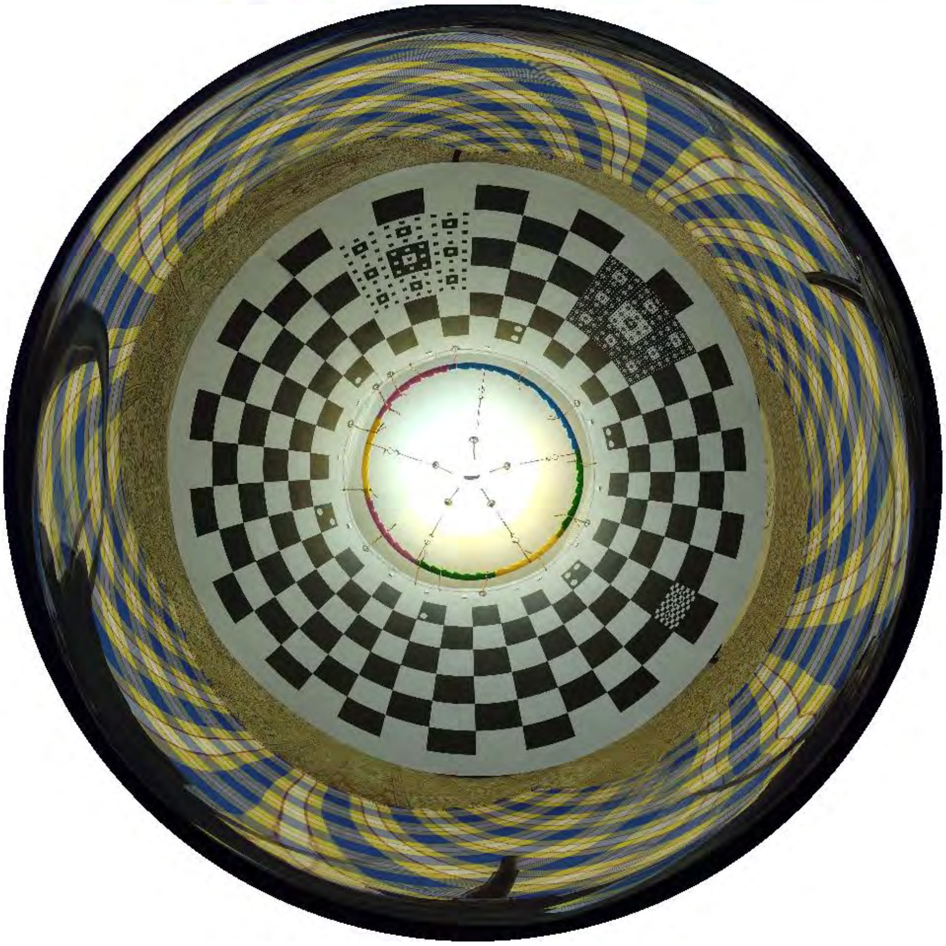

Fig12. The stitched 360º image in the little-planet view

5. Conclusion

The paper proposes a new multi-camera calibration based on the graph pyramid and the novel 360º pattern. It does not assume any geometrical model for the lens distortion of the lenses and therefore can be applied for almost any arbitrary distortion. Morever, the specific design of the emplyed pattern enables it to uniquely encode the 3D world with high resoultion depending of what resolution the camera' set requires. The method also using distance transfoem shift the corners into the center of patches and therefore solves the problem of multi-corner detection happens along the side of the highly distorted image. The future work is to design a colorful version of the pattern and to simulate the non-symmetrical arrangemt of cameras.

References

[1] D. B. Gennery. Generalized camera calibration including fish-eye lenses. IJCV, 68(3):239-266, 2006.
[2] M. Sonka, V. Hlavac, and R. Boyle. Image processing, analysis, and machine vision, 4th Edition. Cengage
Learning, 2014.

[3] R. Swaminathan and S. K. Nayar. Nonmetric calibration of wide-angle lenses and polycameras. IEEE TPAMI, 22(10):1172-1178, 2000.
[4] C. Bräuer-Burchardt and K. Voss. A new algorithm to correct fish-eye- and strong wide-angle-lens-distortion
from single images. In ICIP (1), pages 225-228, 2001.
[5] D. Schneider, E. Schwalbe, and H.-G. Maas. Validation of geometric models for fisheye lenses. ISPRS Journal of Photogrammetry and Remote Sensing, 64(3):259-266, 2009.
[6] S. Abraham and W. Förstner. Fish-eye-stereo calibration and epipolar rectification. ISPRS Journal of photogrammetry and remote sensing, 59(5):278-288, 2005.
[7] S. F. Ray. Applied photographic optics: Lenses and optical systems for photography,film, video, electronic and digital imaging. Focal Press, 2002.
[8] C. Ma, L. Shi, H. Huang, and M. Yan. 3D reconstruction from full-view fisheye camera. arXiv:1506.06273v1 [cs.CV], 2015.
[9] D. Claus and A. W. Fitzgibbon. A rational function lens distortion model for general cameras. In CVPR, volume 1, pages 213-219. IEEE, 2005.
[10] H. Bakstein and T. Pajdla. Panoramic mosaicing with a 180 field of view lens. In Omnidirectional Vision, 2002. Proceedings. Third Workshop on, pages 60-67. IEEE, 2002.
[11] S. Shah and J. Aggarwal. Intrinsic parameter calibration procedure for a (high-distortion) fish-eye lens camera with distortion model and accuracy estimation. Pattern Recognition, 29(11):1775-1788, 1996.
[12] F. Devernay and O. Faugeras. Straight lines have to be straight. MVA, 13(1):14-24, 2001.
[13] P. Srestasathiern and N. Soontranon. A novel camera calibration method for fish-eye lenses using line features. The Int. Arch. of Photogrammetry, Remote Sensing & Spatial Inform. Sciences, 40(3):327, 2014.
[14] E. Antunez, Y. Haxhimusa, R. Marl, W. G. Kropatsch, and A. J. Banderas. Articial visual attention using combinatorial pyramids. In M. Cazorla and J. Garcia-Rodriguez, editors, Robotic Vision: Techn. For ML and Vision Appl., chapter 22, pages 439{457. IGI Global, 2012.
[15]. J. Mallon and P. F. Whelan. Precise radial un-distortion of images. In ICPR, volume 1, pages 18-21. IEEE, 2004.
[16] M. Fleck. Perspective projection: The wrong imaging model. Technical report, Department of Computer Science, University of Iowa, 1995.
[17] P. Sturm and S. Ramalingam. A generic concept for camera calibration. In ECCV, volume LNCS-3022, pages 1-13. Springer, 2004.
[18] M. D. Grossberg and S. K. Nayar. The raxel imaging model and ray-based calibration. IJCV, 61(2):119-137, 2005.
[19] I. Janusch and W. G. Kropatsch. Shape classification according to LBP persistence of critical points. In N. Normand, J. Guedon, and F. Autrusseau, editors, Proc. of the 19th IAPR-TC18 Workshop on Discrete Geometry for Computer Imagery, volume LNCS 9647, pages 166-177. Springer, Berlin Heidelberg, 2016.
[20] L. Quan and Z. Lan. Linear n-point camera pose determination. IEEE TPAMI, 21(8):774-780, 1999.
[21] S. N. Sinha, M. Pollefeys, and L. McMillan. Camera network calibration from dynamic silhouettes. In CVPR, volume 1, pages I-195. IEEE, 2004.
[22] F. Torres and W. G. Kropatsch. Canonical encoding of the combinatorial pyramid. In Z. Kukelova and J. Heller, editors, Proc. of the 19th Computer Vision Winter Workshop, pages 118-125. Czech Society for Cybernetics and Informatics (Czech Pattern Recognition Society group), 2014.
[23] F. Qi, Q. Li, Y. Luo, and D. Hu. Constraints on general motions for camera calibration with one-dimensional objects. Pattern Recognition, 40(6):1785-1792, 2007.

[24] K.-Y. Shin and J. H. Mun. A multi-camera calibration method using a 3-axis frame and wand. Intl. Journal of Precision Engineering and Manufacturing, 13(2):283-289, 2012.
[25] P. Baker and Y. Aloimonos. Complete calibration of a multi-camera network. In Omnidirectional Vision, 2000. Proceedings. IEEE Workshop on, pages 134-141. IEEE, 2000.
[26] Y. Uematsu, T. Teshima, H. Saito, and C. Honghua. D-calib: Calibration software for multiple cameras system. In ICIAP, pages 285-290. IEEE, 2007.
[27] T. Svoboda, D. Martinec, and T. Pajdla. A convenient multicamera self-calibration for virtual environments. Presence, 14(4):407-422, 2005.
[28] Y. Abdel-Aziz, H. Karara, and M. Hauck. Direct linear transformation from comparator coordinates into object space coordinates in close-range photogrammetry. Photogrammetric Engineering & Remote Sensing, 81(2):103-107, 2015.
[29] D. Devarajan, Z. Cheng, and R. J. Radke. Calibrating distributed camera networks. Proceedings of the IEEE, 96(10):1625-1639, 2008.
[30] L. Di Stefano, M. Marchionni, and S. Mattoccia. A fast area-based stereo matching algorithm. Image and vision computing, 22(12):983-1005, 2004.
[31] P. Lebraly, E. Royer, O. Ait-Aider, C. Deymier, and M. Dhome. Fast calibration of embedded nonoverlapping cameras. In ICRA, pages 221-227. IEEE, 2011.
[32] R. K. Kumar, A. Ilie, J.-M. Frahm, and M. Pollefeys. Simple calibration of non-overlapping cameras with a mirror. In CVPR, pages 1-7. IEEE, 2008.
[33] Y. Dai, J. Trumpf, H. Li, N. Barnes, and R. Hartley. Rotation averaging with application to camera-rig calibration. In ACCV 2009, Part II, volume LNCS 5995, pages 335-346. Springer, Berlin Heidelberg, 2010.
[34] R. Szeliski. Image alignment and stitching: A tutorial. Foundations and Trends R in Computer Graphics and Vision, 2(1):1-104, 2006.
[35] J. Zaragoza, T.-J. Chin, M. S. Brown, and D. Suter. As-projective-as-possible image stitching with moving DLT. In ICPR, pages 2339-2346. IEEE, 2013.
[36] J. Kopf, D. Lischinski, O. Deussen, D. Cohen-Or, and M. Cohen. Locally adapted projections to reduce panorama distortions. In Computer Graphics Forum, volume 28, pages 1083-1089. Wiley Online Library, 2009.
[37] M. Z. Brown, D. Burschka, and G. D. Hager. Advances in computational stereo. IEEE TPAMI, 25(8):993-1008, 2003.
[38] D. Scharstein and R. Szeliski. A taxonomy and evaluation of dense two-frame stereo correspondence algorithms. IJCV, 47(1-3):7-42, 2002.
[39] D. N. Bhat and S. K. Nayar. Ordinal measures for image correspondence. IEEE TPAMI, 20(4):415-423, 1998.
[40] V. S. Kluth, G. W. Kunkel, and U. A. Rauhala. Global least squares matching. In Geoscience and Remote Sensing Symposium, 1992. IGARSS'92. Intl., volume 2, pages 1615-1618. IEEE, 1992.
[41] C. Schmid and A. Zisserman. The geometry and matching of lines and curves over multiple views. IJCV, 40(3):199-233, 2000.
[42] S. Birchfield and C. Tomasi. Depth discontinuities by pixel-to-pixel stereo. IJCV, 35(3):269-293, 1999.
[43] C. Tomasi and R. Manduchi. Stereo matching as a nearest-neighbor problem. IEEE TPAMI, 20(3):333-340, 1998.
[44] V. Kolmogorov and R. Zabih. Computing visual correspondence with occlusions using graph cuts. In ICCV, volume 2, pages 508-515. IEEE, 2001.
[45] L. Di Stefano, M. Marchionni, and S. Mattoccia. A fast area-based stereo matching algorithm. Image and vision computing, 22(12):983-1005, 2004.

[46] C. L. Zitnick and T. Kanade. A cooperative algorithm for stereo matching and occlusion detection. IEEE TPAMI, 22(7):675-684, 2000.
[47] W. G. Kropatsch. Equivalent contraction kernels to build dual irregular pyramids. Advances in Computer Science, Advances in Computer Vision:pp. 99-107, 1997.
[48] M. Banaeyan, H. Huber, W. Kropatsch, and R. Barth. A novel concept for smart camera image stitching. In L. Cehovin, R. Mandeljc, and V. Struc, editors, Proc. of the 21st Computer Vision Winter Workshop. Slovenian Pattern Recognition Society, Ljubljana, 2016.